Contributors

E.H. Aassif LMTI, Faculty of Science, Ibn Zohr University, Agadir, Morocco, aassifh@menara.ma

L. Airoldi School of Aerospace Engineering, Georgia Institute of Technology, Atlanta, USA, luca.airoldi@gatech.edu

R. Akkerman Engineering Technology, Production Technology, University of Twente, P.O. Box 217, 7500AE, Enschede, The Netherlands, r.akkerman@utwente.nl

B. Beck G.W. Woodruff School of Mechanical Engineering, Georgia Institute of Technology, Atlanta, USA, benbeck@gatech.edu

J. Belinha Institute of Mechanical Engineering—IDMEC, Rua Dr. Roberto Frias, 4200-465 Porto, Portugal, jorge.belinha@fe.up.pt

A. de Boer Engineering Technology, Applied Mechanics and Acoustics, University of Twente, P.O. Box 217, 7500AE, Enschede, The Netherlands, a.deboer@utwente.nl

L.C. Cardoso INEGI, Universidade do Porto, Campus da FEUP, R. Dr. Roberto Frias 400, 4200-465 Porto, Portugal, luis.carlos.cardoso@fe.up.pt

F. Casadei School of Aerospace Engineering, Georgia Institute of Technology, Atlanta, USA, filippo.casadei@gatech.edu

G. Cazzulani Mechanical Engineering Department, Politecnico di Milano, Via La Masa 1, 20156 Milan, Italy, gabriele.cazzulani@mail.polimi.it

M. Collet Department of Applied Mechanics, FEMTO-ST UMR 6174, Besançon, France, manuel.collet@univ-fcomte.fr

K.A. Cunefare G.W. Woodruff School of Mechanical Engineering, Georgia Institute of Technology, Atlanta, USA, ken.cunefare@me.gatech.edu

L.M.J.S. Dinis Faculty of Engineering of the University of Porto—FEUP, Rua Dr. Roberto Frias, 4200-465 Porto, Portugal, ldinis@fe.up.pt

M. Ferrari Mechanical Engineering Department, Politecnico di Milano, Via La Masa 1, 20156 Milan, Italy, matteo.ferrari@mail.polimi.it

E. Foltête FEMTO-ST Institute, Applied Mechanics, University of Franche-Comté, 25000 Besançon, France, emmanuel.foltete@univ-fcomte.fr

C. Ghielmetti Mechanical Engineering Department, Politecnico di Milano, Via La Masa 1, 20156 Milan, Italy, christian.ghielmetti@mecc.polimi.it

H. Giberti Mechanical Engineering Department, Politecnico di Milano, Via La Masa 1, 20156 Milan, Italy, hermes.giberti@polimi.it

L. Gil Espert Laboratori per a la Innovació Tecnològica d'Estructures i Materials, Universitat Politècnica de Catalunya, C/Colon, 11 TR45, 08225 Terrassa, Barcelona, Spain, lluis.gil@upc.edu

M. Laaboubi LMTI, Faculty of Science, Ibn Zohr University, Agadir, Morocco, laaboubi@gmail.com

A.A. Lakis École Polytechnique, Montréal, QC, H3C 3A7, Canada, ouni.lakis@polymtl.ca

R. Latif ESSI, National School of Applied Science, Ibn Zohr University, Agadir, Morocco, latif@ensa-agadir.ac.ma

R. Loendersloot Engineering Technology, Applied Mechanics and Acoustics, University of Twente, P.O. Box 217, 7500AE, Enschede, The Netherlands, r.loendersloot@utwente.nl

L. Marcouiller Institut de Recherche Hydro Québec, Varennes, QC, J3X 1S1, Canada, marcouiller.luc@ireq.ca

G. Maze LOMC, Le Havre University, Le Havre, France, gerard.maze@univ-lehavre.fr

R.M. Natal Jorge Faculty of Engineering of the University of Porto—FEUP, Rua Dr. Roberto Frias, 4200-465 Porto, Portugal, rnatal@fe.up.pt

T.H. Ooijevaar Engineering Technology, Production Technology, University of Twente, P.O. Box 217, 7500AE, Enschede, The Netherlands, t.h.ooijevaar@utwente.nl

M. Ouisse Department of Applied Mechanics, FEMTO-ST UMR 6174, Besançon, France; FEMTO-ST Institute, Applied Mechanics, University of Franche-Comté, 25000 Besançon, France, morvan.ouisse@univ-fcomte.fr

M.A. Pérez Martínez Department of Strength of Materials and Structures, Universitat Politècnica de Catalunya, C/Colon, 11 TR45, 08225 Terrassa, Barcelona, Spain, marco.antonio.perez@upc.edu

P. Poletti Department of Sonology, Escola Superior de Música de Catalunya, C/Padilla, 155, 08013 Barcelona, Spain, paul@polettipiano.com

F. Resta Mechanical Engineering Department, Politecnico di Milano, Via La Masa 1, 20156 Milan, Italy, ferruccio.resta@polimi.it

F. Ripamonti Mechanical Engineering Department, Politecnico di Milano, Via La Masa 1, 20156 Milan, Italy, francesco.ripamonti@polimi.it

M. Ruzzene School of Aerospace Engineering, Georgia Institute of Technology, Atlanta, USA, massimo.ruzzene@aerospace.gatech.edu

A.S. Sarıgül Department of Mechanical Engineering, Dokuz Eylül University, 35100 Bornova, Izmir, Turkey, saide.sarigul@deu.edu.tr

A. Seçgin Department of Mechanical Engineering, Dokuz Eylül University, 35100 Bornova, Izmir, Turkey, abdullah.secgin@deu.edu.tr

M. Thomas École de Technologie Supérieure, 1100 Notre Dame West, Montréal, QC, H3C 1K3, Canada, marc.thomas@etsmtl.ca

C.M.A. Vasques INEGI, Universidade do Porto, Campus da FEUP, R. Dr. Roberto Frias 400, 4200-465 Porto, Portugal, cmav@fe.up.pt

V.-H. Vu École de Technologie Supérieure, 1100 Notre Dame West, Montréal, QC, H3C 1K3, Canada, viethung.vu.1@ens.etsmtl.ca

L. Warnet Engineering Technology, Production Technology, University of Twente, P.O. Box 217, 7500AE, Enschede, The Netherlands, l.warnet@utwente.nl

Chapter 11
Identification of Reduced Models from Optimal Complex Eigenvectors in Structural Dynamics and Vibroacoustics

M. Ouisse and E. Foltête

Abstract The objective of this chapter is to present some efficient techniques for identification of reduced models from experimental modal analysis in the fields of structural dynamics and vibroacoustics. The main objective is to build mass, stiffness and damping matrices of an equivalent system which exhibits the same behavior as the one which has been experimentally measured. This inverse procedure is very sensitive to experimental noise and instead of using purely mathematical regularization techniques, physical considerations can be used. Imposing the so-called properness condition of complex modes on identified vectors leads to matrices which have physical meanings and whose behavior is as close as possible to the measured one. Some illustrations are presented on structural dynamics. Then the methodology is extended to vibroacoustics and illustrated on measured data.

11.1 Introduction

Being able to identify reduced physical models can help designers to understand the behavior of the system in a given frequency range, and orient design decisions in order to reach a given objective. Performing model reduction is quite usual in the field of numerical analysis [14, 29], in this case the objective is to find a model with a reduced number of degrees of freedom, which can be deduced from a large model, in order that the reduced model exhibits the same behavior as the full one in a frequency band of interest. An alternative to this model-based methodology could be based on experimental measurements. The basic idea is to identify from measurements the matrices describing the behavior of the system in order to help the designer to make proper decisions. The main difficulty in this kind of analysis is related to the very bad conditioning of the inverse procedure, since experimental conditions induce noise in the data, resulting in large changes in the final identified system matrices, in particular for the damping terms.

M. Ouisse (✉) · E. Foltête
FEMTO-ST Institute, Applied Mechanics, University of Franche-Comté, 25000 Besançon, France
e-mail: morvan.ouisse@univ-fcomte.fr

E. Foltête
e-mail: emmanuel.foltete@univ-fcomte.fr

C.M.A. Vasques, J. Dias Rodrigues (eds.), *Vibration and Structural Acoustics Analysis*,
DOI 10.1007/978-94-007-1703-9_11, © Springer Science+Business Media B.V. 2011

Book ID: 270321_1_En, Date: 2011-07-07, UNCORRECTED PROOF

Several approaches have been proposed throughout the last decades to regularize the inverse problem on the field of structural dynamics. A brief overview of the state of the art is given in Sect. 11.2. Section 11.3 is dedicated to the so-called properness condition for structural dynamics and can be considered as a tutorial section. Original illustrations are presented to help the reader to understand the importance of the condition. An experimental test-case is given to illustrate application of the methodology on a real structure, on which a reduced model is directly derived from the experimental data. In Sect. 11.4, the properness condition is extended to vibroacoustics and new results about optimal correction of vibroacoustic complex modes are given. Several corrections techniques are described and illustrated on experimental data coming from vibroacoustic measurements on a guitar. Section 11.5 is dedicated to prospectives: some comments are given about the structural dynamics applications of the methodology, and some suggestions are given for improvement of the methodology concerning vibroacoustic applications. Section 11.6 gives some conclusions and a summary of the work presented in this chapter. The bibliography and a selection of additional references are finally given at the end of the chapter.

11.2 Overview of the State of the Art

Identification of analytical models from measurements in structural dynamics is still an open question, in particular concerning the damping terms. Both stiffness and mass can be derived quite easily from models, or even from experiments with reasonable confidence. As far as the dissipative effects are concerned, there is still no consensus about the most reliable technique to obtain a physical description of damping which can be efficient for simulation.

In this chapter we will mainly focus on techniques based on experimental data, that allow identification of second-order matrices corresponding to classical stiffness, mass and viscous damping terms of multi-degrees of freedom models. This topic has shown a growing interest over the last decades. The fundamental book from Lord Rayleigh [34] includes some considerations about sensitivity of eigenfrequencies and eigenvectors which are of first interest for system identification. Damping aspects have been at the center of several works, among which the famous papers from Caughey [11] including considerations about normal and complex modes, which are of first importance in the context of interest.

Some review papers have been published [10, 15, 20], including many references to important works on damping related aspects. More recently, some papers have focused on the particular case of damping identification from measurement [33, 35, 36]. In these papers, the authors exhibit a large set of available methods, starting either from Frequency Response Functions (FRFs) or modal data to identify at least the damping matrix. These methods are applied and compared on given test-cases. An interesting point is that these papers do not lead to the same conclusions concerning the efficiency of the techniques for practical applications, which clearly means that there is still some work to do, even if among the available methods, some of them can provide quite confident results.

One of the ways to obtain the system matrices is to start from identified complex modes. This chapter will be limited to this case, and will focus on a particular point, called properness condition, which is not addressed in the review papers referenced above. This condition, which has been mentioned in several publications [9, 22, 24, 41], is automatically verified by the exact complex modes of the system. When a full basis is extracted from experimental data to reconstruct a physical model, this condition should be enforced on the complex modes to obtain physical results. Balmès [7] has proposed a methodology to find optimal complex vectors which are as close as possible as initial identified vectors, while verifying the properness condition. Another way to obtain optimal complex vectors from measured ones has been proposed by Adhikari [1], but this method requires the knowledge of real modes, which is not necessarily the case in practical applications.

11.3 Properness Condition in Structural Dynamics

The very classical matrix formulation used for structural dynamics is

$$\mathbf{M}\ddot{\mathbf{q}}(t) + \mathbf{C}\dot{\mathbf{q}}(t) + \mathbf{K}\mathbf{q}(t) = \mathbf{f}(t), \tag{11.1}$$

where $\mathbf{q}(t)$ is the vector of generalized displacements of the structure, $\mathbf{M}$ is the mass matrix of the structure, $\mathbf{K}$ is the stiffness matrix of the structure, $\mathbf{C}$ represents viscous losses and $\mathbf{f}(t)$ is the vector representing the generalized forces on the structure. One way to solve the system in Eq. (11.1) for steady-state harmonics is to use modal decomposition. This can be done using the space-state representation of the system,

$$\mathbf{U}\dot{\mathbf{Q}}(t) - \mathbf{A}\mathbf{Q}(t) = \mathbf{F}(t), \tag{11.2}$$

where

$$\mathbf{U} = \begin{bmatrix} \mathbf{C} & \mathbf{M} \\ \mathbf{M} & \mathbf{0} \end{bmatrix}, \quad \mathbf{A} = \begin{bmatrix} -\mathbf{K} & \mathbf{0} \\ \mathbf{0} & \mathbf{M} \end{bmatrix}, \quad \mathbf{Q}(t) = \begin{Bmatrix} \mathbf{q}(t) \\ \dot{\mathbf{q}}(t) \end{Bmatrix}, \quad \mathbf{F}(t) = \begin{Bmatrix} \mathbf{f}(t) \\ \mathbf{0} \end{Bmatrix}. \tag{11.3}$$

The eigenvalues of this problem can be stored in the spectral matrix $\mathbf{\Lambda}$, so that

$$\mathbf{\Lambda} = \left[^{\diagdown} \lambda_j {}_{\diagdown} \right]. \tag{11.4}$$

The j-th eigenvalue is associated to the eigenvector $\boldsymbol{\theta}_j$ such as $(\mathbf{U}\lambda_j - \mathbf{A})\boldsymbol{\theta}_j = \mathbf{0}$, where $\boldsymbol{\theta}_j = \{\boldsymbol{\psi}_j^{\mathrm{T}}\ \boldsymbol{\psi}_j^{\mathrm{T}}\lambda_j\}^{\mathrm{T}}$, $\boldsymbol{\psi}_j$ being the complex eigenvector in the physical space (i.e. its components are related to $\mathbf{q}$). Storing the eigenvectors (in the same order as the eigenvalues) in the modal matrix $\mathbf{\Theta} = [\mathbf{\Psi}^{\mathrm{T}}\ \mathbf{\Lambda}\mathbf{\Psi}^{\mathrm{T}}]^{\mathrm{T}}$, the following relationship is verified:

$$\mathbf{U}\mathbf{\Theta}\mathbf{\Lambda} = \mathbf{A}\mathbf{\Theta}. \tag{11.5}$$

The orthogonality relationships can be written using $2n$ arbitrary values to build the diagonal matrix $\boldsymbol{\xi} = [\diagdown \xi_j \diagdown]$,

$$\boldsymbol{\Theta}^{\mathrm{T}}\mathbf{U}\boldsymbol{\Theta} = \boldsymbol{\xi} \quad \text{or} \quad \boldsymbol{\Theta}^{\mathrm{T}}\mathbf{A}\boldsymbol{\Theta} = \boldsymbol{\xi}\boldsymbol{\Lambda}. \tag{11.6}$$

The modal decomposition of the permanent harmonic response at frequency ω is finally

$$\mathbf{Q}(t) = \boldsymbol{\Theta}\big(\boldsymbol{\xi}(\mathrm{i}\omega\mathbf{E}_{2n} - \boldsymbol{\Lambda})\big)^{-1}\boldsymbol{\Theta}^{\mathrm{T}}\mathbf{F}(\omega)e^{\mathrm{i}\omega t}, \tag{11.7}$$

where $\mathbf{E}_{2n}$ is a $2n \times 2n$ identity matrix and $\mathbf{F}(\omega)$ is the complex amplitude of the harmonic excitation. This relationship can also be written using the n degrees of freedom notation in the frequency domain as

$$\mathbf{q}(\omega) = \boldsymbol{\Psi}\,\Xi\,\boldsymbol{\Psi}^{\mathrm{T}}\mathbf{f}(\omega), \tag{11.8}$$

where

$$\Xi = \left[\diagdown \frac{1}{\xi_j(\mathrm{i}\omega - \lambda_j)} \diagdown\right]. \tag{11.9}$$

In the following, without loss of generality, the eigenshapes are supposed to be normalized such as $\xi_j = 1$.

11.3.1 Properness of Complex Modes

The properness condition is related to the inverse procedure: starting from the modal basis, the orthogonality relationships can be inverted to obtain the system matrices. Inverting relationships (11.6) leads to

$$\mathbf{U}^{-1} = \boldsymbol{\Theta}\boldsymbol{\Theta}^{\mathrm{T}}, \tag{11.10}$$

or

$$\begin{aligned}\begin{bmatrix} \mathbf{C} & \mathbf{M} \\ \mathbf{M} & \mathbf{0} \end{bmatrix}^{-1} &= \begin{bmatrix} \mathbf{0} & \mathbf{M}^{-1} \\ \mathbf{M}^{-1} & -\mathbf{M}^{-1}\mathbf{C}\mathbf{M}^{-1} \end{bmatrix} \\ &= \begin{bmatrix} \boldsymbol{\Psi}\boldsymbol{\Psi}^{\mathrm{T}} & \boldsymbol{\Psi}\boldsymbol{\Lambda}\boldsymbol{\Psi}^{\mathrm{T}} \\ \boldsymbol{\Psi}\boldsymbol{\Lambda}\boldsymbol{\Psi}^{\mathrm{T}} & \boldsymbol{\Psi}\boldsymbol{\Lambda}^2\boldsymbol{\Psi}^{\mathrm{T}} \end{bmatrix},\end{aligned} \tag{11.11}$$

and

$$\mathbf{A}^{-1} = \boldsymbol{\Theta}\boldsymbol{\Lambda}\boldsymbol{\Theta}^{\mathrm{T}}, \tag{11.12}$$

or

$$\begin{aligned}\begin{bmatrix} -\mathbf{K} & \mathbf{0} \\ \mathbf{0} & \mathbf{M} \end{bmatrix}^{-1} &= \begin{bmatrix} -\mathbf{K}^{-1} & \mathbf{0} \\ \mathbf{0} & \mathbf{M}^{-1} \end{bmatrix} \\ &= \begin{bmatrix} \boldsymbol{\Psi}\boldsymbol{\Lambda}^{-1}\boldsymbol{\Psi}^{\mathrm{T}} & \boldsymbol{\Psi}\boldsymbol{\Psi}^{\mathrm{T}} \\ \boldsymbol{\Psi}\boldsymbol{\Psi}^{\mathrm{T}} & \boldsymbol{\Psi}\boldsymbol{\Lambda}\boldsymbol{\Psi}^{\mathrm{T}} \end{bmatrix}.\end{aligned} \tag{11.13}$$

From these expressions, the mass, stiffness and damping matrices can be expressed as

$$\mathbf{M} = \left[\boldsymbol{\Psi}\boldsymbol{\Lambda}\boldsymbol{\Psi}^{\mathrm{T}}\right]^{-1}, \tag{11.14}$$

$$\mathbf{K} = -\left[\boldsymbol{\Psi}\boldsymbol{\Lambda}^{-1}\boldsymbol{\Psi}^{\mathrm{T}}\right]^{-1}, \tag{11.15}$$

$$\mathbf{C} = -\left[\mathbf{M}\boldsymbol{\Psi}\boldsymbol{\Lambda}^{2}\boldsymbol{\Psi}^{\mathrm{T}}\mathbf{M}\right]. \tag{11.16}$$

These relationships are only valid if the complex modes verify the properness condition that directly comes from the zero terms in inverse matrices:

$$\boldsymbol{\Psi}\boldsymbol{\Psi}^{\mathrm{T}} = \mathbf{0}. \tag{11.17}$$

It should be emphasized that this methodology leads to identification of matrices only if all modes of the system are identified. This is of course not realistic for continuous structures. Nevertheless, the reconstruction equations can lead to useful condensed model of the continuous structure if the number of identified modes is equal to the number of measured degrees of freedom, and if the locations of the sensors ensures physical meaning for the degrees of freedom of the reduced model. Some techniques are available to provide estimation of matrices when only a subset of the modes are identified, or even directly from measured FRFs. The readers are invited to refer to corresponding papers [12, 19, 21, 26, 28] or reviews [33, 35, 36] for more details. This chapter is limited to model reconstruction from a full set of complex modes.

11.3.2 Illustration of Properness Impact on Inverse Procedure

When dealing with experimental data for matrices identification, it is clear that the input data (i.e. the complex eigenshapes) are polluted with random noise. In order to illustrate that point, a numerical example can be used: starting from exact solutions of a 4 degrees-of-freedom system, the eigenshapes are modified using a random noise of growing amplitude acting on amplitude and phase of vectors. This numerical noise does not necessarily represent exactly experimental noise, it is used here for a sake of simplicity, in order to illustrate impact of noise on properness condition. Experimental results will be shown later, on which the trends observed here will be confirmed.

Figure 11.1 shows the impact of noise on the properness norm. The norm which is used here is the norm 2, i.e. the largest singular value of the matrix.

It can clearly be observed that the properness norm grows up with the noise on inputs, which means that the inverse relations are no longer valid as soon as the properness condition is not verified. This is confirmed by Fig. 11.2, which shows the error on identified matrices, this error being defined from the ratio of norm 2 of the difference between identified and exact matrices to the norm 2 of the exact

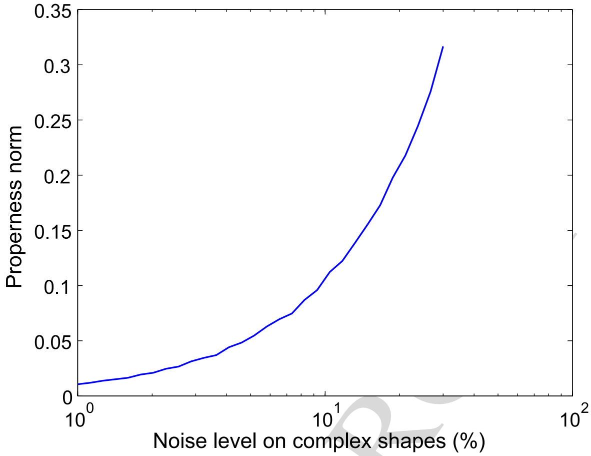

Fig. 11.1 Impact of noise on eigenvectors on properness norm

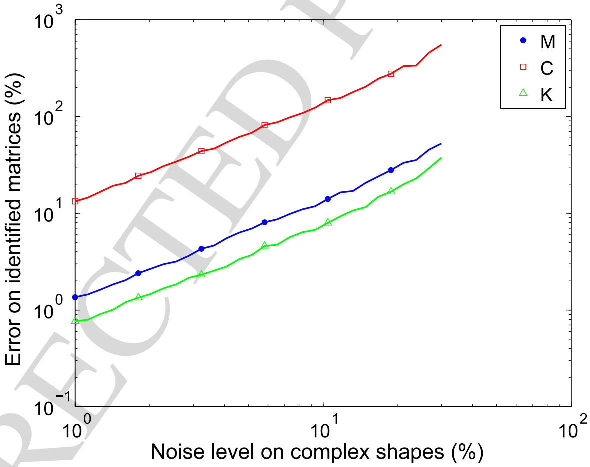

Fig. 11.2 Impact of noise on eigenvectors on error on identified matrices

matrices. It is clear from the figure that some very large errors can be obtained on matrices identification for small errors levels on inputs, in particular for the damping identification, while the identification of mass and stiffness matrices is quite robust, i.e. the level of error on outputs is of the same order as the level of error on inputs. Proper complex modes are then of first importance for correct damping estimation.

11.3.3 Properness Enforcement

When the complex modes are available from experimental identification, Eqs. (11.14)–(11.16) can be used in order to find the reduced model which is supposed to have the same behavior as the measured system. In general, the complex modes do not verify the properness condition (11.17) and Ref. [7] proposes a

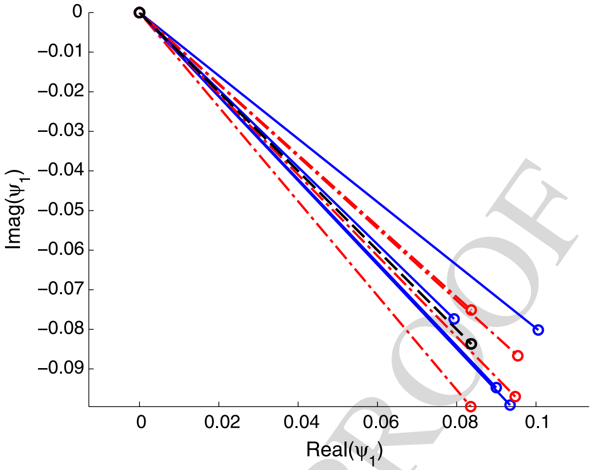

Fig. 11.3 Eigenvectors of the first mode in complex plane: initial shapes (*dashed line*), modified shapes (*continuous line*) and proper shapes (*dashdot line*)

methodology to enforce properness condition, in order to obtain optimal complex modes. The objective is to find the approximate complex vectors, which are as close as possible to the identified ones, and that verify the properness condition. It is shown that for structural dynamics, an explicit solution can be found, requiring only to solve a Riccati equation. This equation can be deduced from the problem

$$\text{Find } \tilde{\boldsymbol{\Psi}} \text{ minimizing } \|\tilde{\boldsymbol{\Psi}} - \boldsymbol{\Psi}\| \text{ while } \tilde{\boldsymbol{\Psi}}\tilde{\boldsymbol{\Psi}}^{\mathrm{T}} = \mathbf{0}. \tag{11.18}$$

Writing this problem using a constrained minimization approach leads to

$$\tilde{\boldsymbol{\Psi}} = [\mathbf{E}_n - \boldsymbol{\delta}\bar{\boldsymbol{\delta}}]^{-1}[\boldsymbol{\Psi} - \boldsymbol{\delta}\overline{\boldsymbol{\Psi}}], \tag{11.19}$$

where $\boldsymbol{\delta}$ is a Lagrange multiplier matrix, that can be found by solving the Riccati equation

$$\boldsymbol{\Psi}\boldsymbol{\Psi}^{\mathrm{T}} - \boldsymbol{\delta}\overline{\boldsymbol{\Psi}}\boldsymbol{\Psi}^{\mathrm{T}} - \boldsymbol{\Psi}\overline{\boldsymbol{\Psi}}^{\mathrm{T}}\boldsymbol{\delta} + \boldsymbol{\delta}\overline{\boldsymbol{\Psi}}\,\overline{\boldsymbol{\Psi}}^{\mathrm{T}}\boldsymbol{\delta} = \mathbf{0}. \tag{11.20}$$

In the previous equations, $\overline{\boldsymbol{\Psi}}$ is the conjugate of $\boldsymbol{\Psi}$. After properness enforcement, the eigenvectors are typically mainly changed in phase, while the amplitude of vectors remains almost the same, as shown in Figs. 11.3, 11.4, 11.5 and 11.6, which present the eigenvectors of the four modes in complex plane. The figure exhibits three families of shapes:

– the initial shapes, corresponding to those of the initial system;
– the modified shapes, obtained after random changes of initial shapes;
– the proper shapes, deduced from the modified ones after properness enforcement.

It is quite clear from this picture that the proper modes are not those of the initial system, but the closest ones to modified ones that verify the properness condition. The case considered here for illustration is undoubtedly an extreme case, since it corresponds to the highest value of random noise used in Figs. 11.1 and 11.2, i.e. 30% in amplitude and phase. For practical applications, lower level of noise is expected, and the starting vectors should be closer to the "true" shapes of the system.

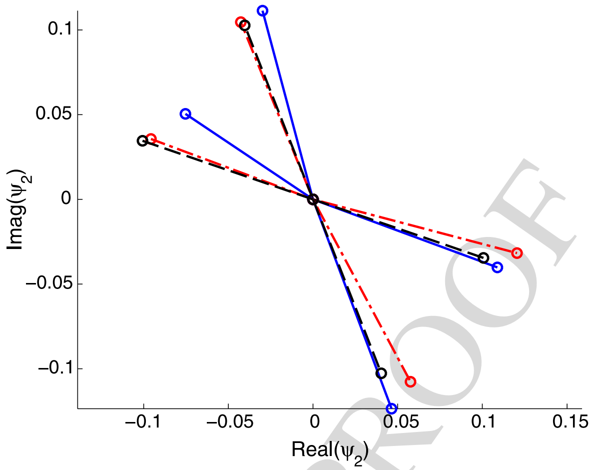

Fig. 11.4 Eigenvectors of the second mode in complex plane: initial shapes (*dashed line*), modified shapes (*continuous line*) and proper shapes (*dashdot line*)

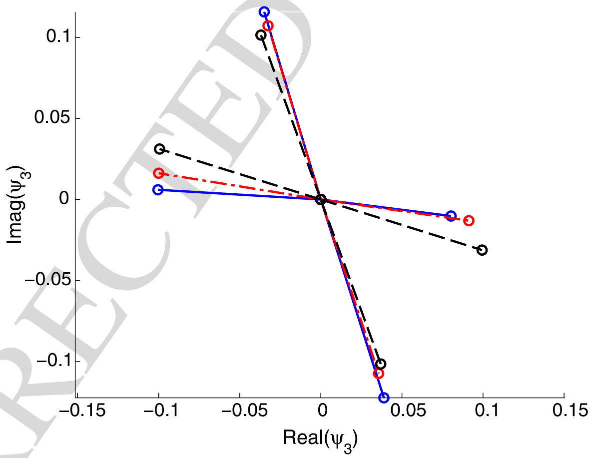

Fig. 11.5 Eigenvectors of the third mode in complex plane: initial shapes (*dashed line*), modified shapes (*continuous line*) and proper shapes (*dashdot line*)

In order to obtain the characteristic matrices of formulation (11.1), one has then to consider the following steps:

- build FRFs from time domain measurements;
- use complex curve fitting in order to find the complex modes in the frequency range of interest [17, 38];
- use the properness enforcement technique to obtain modified complex eigenvectors from identified ones;
- use inverse relationships (11.14) to (11.16) to find the matrices of formulation (11.1).

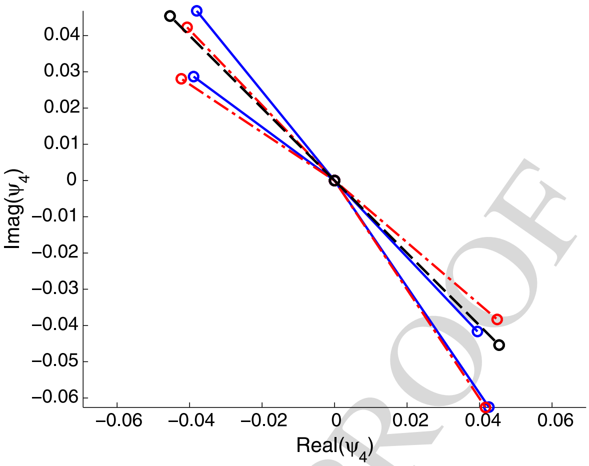

Fig. 11.6 Eigenvectors of the fourth mode in complex plane: initial shapes (*dashed line*), modified shapes (*continuous line*) and proper shapes (*dashdot line*)

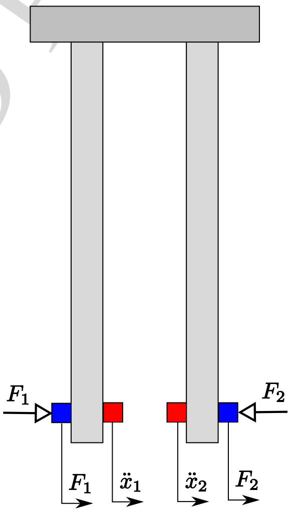

Fig. 11.7 Experimental test-case: two bending beams coupled by common clamping device

11.3.4 Experimental Illustration

In this section an experimental illustration of the methodology is presented. Figure 11.7 shows the experimental set-up which has been used. It is constituted with two bending beams which are coupled through their bases by a common “clamping” device. The frequency range of interest concerns the two firsts modes of the coupled system, which could be represented by a 2-degrees of freedom equivalent model, using points 1 and 2 indicated in Fig. 11.7 as reference points. These points are equipped with accelerometers and some contactless force transducers are used to excite the structure, with force sensors. An electrical intensity probe has also been used to check the value of the force sensors and to verify that the moving masses do not perturb the measured information.

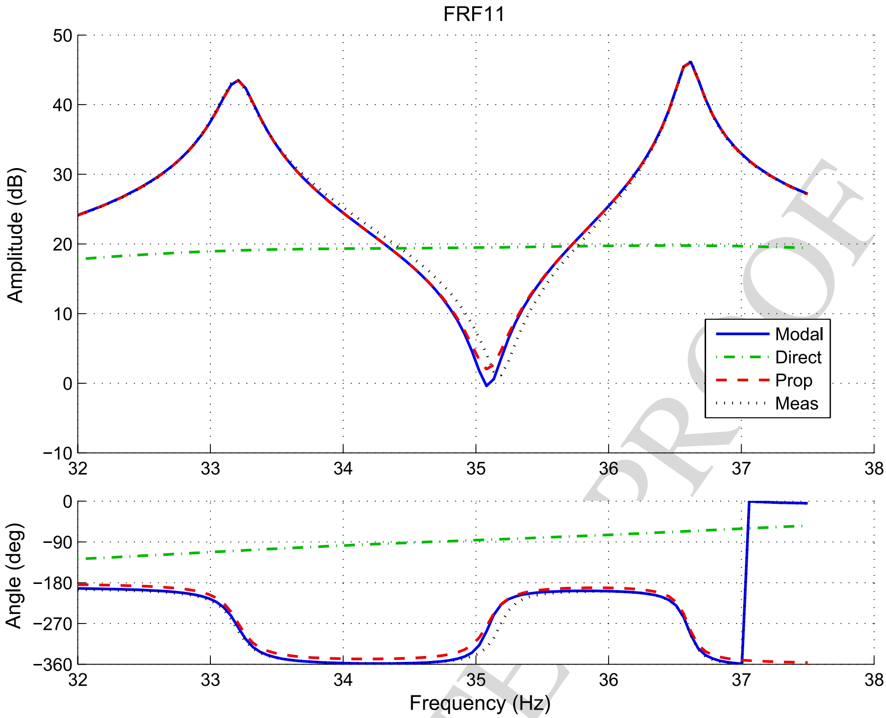

Fig. 11.8 Comparison of measured and synthesized FRF11

The complex eigenvectors which have been identified from the experimental FRFs are

$$\boldsymbol{\Psi} = \begin{bmatrix} 0.0324 - 0.0377\mathrm{i} & 0.0283 - 0.0328\mathrm{i} \\ 0.0249 - 0.0303\mathrm{i} & -0.0298 + 0.0350\mathrm{i} \end{bmatrix}. \tag{11.21}$$

The matrices which are deduced from original vectors are

$$\mathbf{M} = \begin{bmatrix} 0.5360 & 0.0348 \\ 0.0348 & 0.6320 \end{bmatrix}, \tag{11.22}$$

$$\mathbf{C} = \begin{bmatrix} -17.0 & -1.29 \\ -1.29 & -23.7 \end{bmatrix}, \tag{11.23}$$

$$\mathbf{K} = \begin{bmatrix} 2.53 \times 10^4 & -1.00 \times 10^3 \\ -1.00 \times 10^3 & 3.07 \times 10^4 \end{bmatrix}. \tag{11.24}$$

It is clear that the identified damping matrix is not physical. In order to improve its identification, the properness condition is enforced on the complex vectors

$$\tilde{\boldsymbol{\Psi}} = \begin{bmatrix} 0.0352 - 0.0349\mathrm{i} & 0.0304 - 0.0307\mathrm{i} \\ 0.0275 - 0.0277\mathrm{i} & -0.0325 + 0.0323\mathrm{i} \end{bmatrix}. \tag{11.25}$$

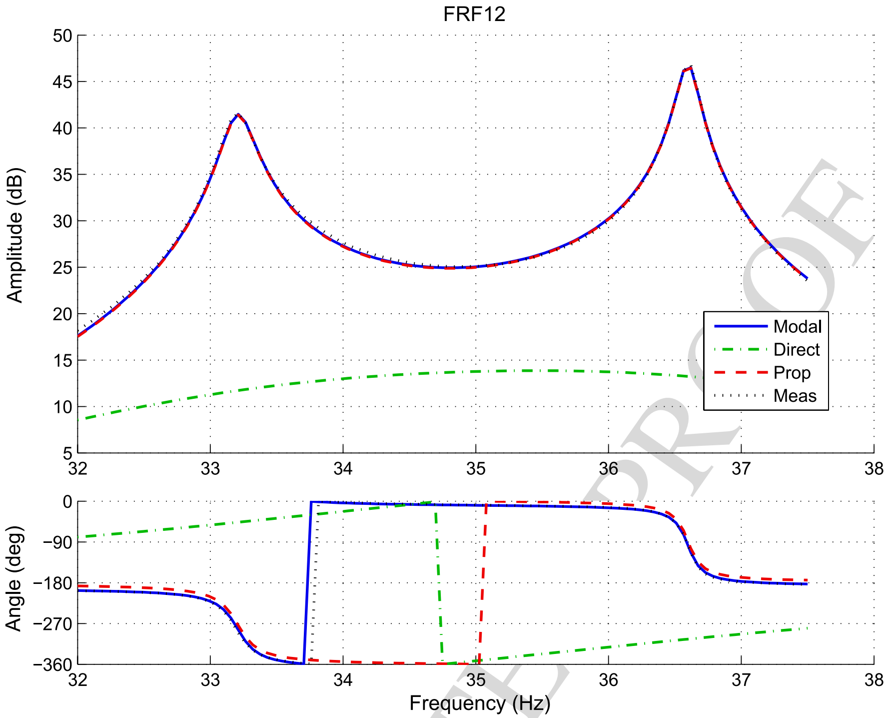

Fig. 11.9 Comparison of measured and synthesized FRF12

The amount of change in these vectors is clearly in the same order of magnitude as the one observed in the numerical illustration. These small changes in vectors clearly improve the matrices identification

$$\tilde{\mathbf{M}} = \begin{bmatrix} 0.5330 & 0.0343 \\ 0.0343 & 0.6270 \end{bmatrix}, \tag{11.26}$$

$$\tilde{\mathbf{C}} = \begin{bmatrix} 0.569 & 0.194 \\ 0.194 & 0.848 \end{bmatrix}, \tag{11.27}$$

$$\tilde{\mathbf{K}} = \begin{bmatrix} 2.52 \times 10^4 & -1.02 \times 10^3 \\ -1.02 \times 10^3 & 3.05 \times 10^4 \end{bmatrix}. \tag{11.28}$$

Changes associated to properness enforcement have a very limited impact on mass and stiffness identification, while they have a strong effect on the damping identification. The first observation that can be done is related to the numerical values in the damping matrix, which correspond to possible physical values. The second observation is that the identified values with properness enforcement are in accordance with the measured data, as indicated in Figs. 11.8, 11.9 and 11.10. These figures show the measured FRFs, the synthesized FRFs from complex modes

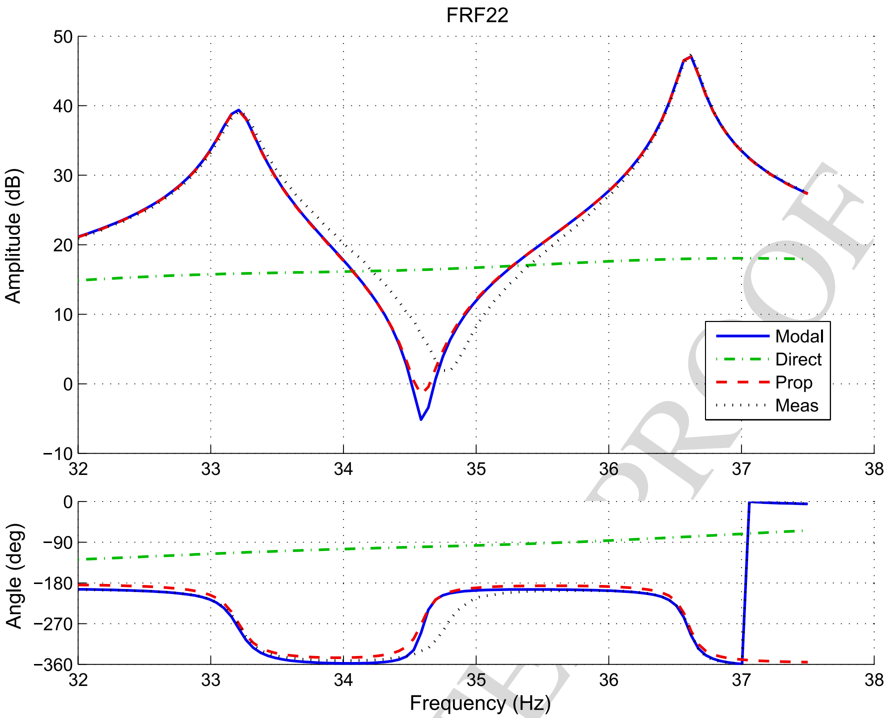

Fig. 11.10 Comparison of measured and synthesized FRF22

identified using a curve fitting technique, the synthesized FRFs obtained from direct calculation using matrices coming from identified complex modes, and the corresponding ones after properness enforcement.

The figures clearly show that:

– the initial modal identification seems to be correct, since the associated synthesized FRFs are very close to the measured one;
– if these identified modes are used for matrices identification, the bad conditioning of the problem leads to very large errors (as indicated above, mainly due to bad damping identification);
– if these modes are slightly modified in accordance with the properness condition, the identified matrices are able to represent the behavior of the measured structure.

For damping identification purposes, it is then clear that properness enforcement on complex vectors must be considered. This operation can be seen as a regularization technique based on physical considerations, instead of using purely mathematical methods. The procedure to enforce properness has been proposed some years ago [7], but unfortunately it is not widely used as it should be. The next section is dedicated to extension of properness for vibroacoustics.

11.4 Extension of Properness to Vibroacoustics

11.4.1 Equations of Motion

Discretizing an internal vibroacoustical problem using the natural fields for the description of the structure (those which can be directly measured), i.e. displacement for the structure and acoustic pressure for the cavity, leads to the matrix system [29]

$$\underbrace{\begin{bmatrix} \mathbf{M}_s & \mathbf{0} \\ \mathbf{L}^{\mathrm{T}} & \mathbf{M}_a \end{bmatrix}}_{\mathbf{M}} \underbrace{\begin{Bmatrix} \ddot{\mathbf{x}}(t) \\ \ddot{\mathbf{p}}(t) \end{Bmatrix}}_{\ddot{\mathbf{q}}(t)} + \underbrace{\begin{bmatrix} \mathbf{C}_s & \mathbf{0} \\ \mathbf{0} & \mathbf{C}_a \end{bmatrix}}_{\mathbf{C}} \underbrace{\begin{Bmatrix} \dot{\mathbf{x}}(t) \\ \dot{\mathbf{p}}(t) \end{Bmatrix}}_{\dot{\mathbf{q}}(t)} + \underbrace{\begin{bmatrix} \mathbf{K}_s & -\mathbf{L} \\ \mathbf{0} & \mathbf{K}_a \end{bmatrix}}_{\mathbf{K}} \underbrace{\begin{Bmatrix} \mathbf{x}(t) \\ \mathbf{p}(t) \end{Bmatrix}}_{\mathbf{q}(t)} = \underbrace{\begin{Bmatrix} \mathbf{F}_s(t) \\ \dot{\mathbf{Q}}_a(t) \end{Bmatrix}}_{\mathbf{f}(t)}, \tag{11.29}$$

where $\mathbf{x}(t)$ is the vector of generalized displacements of the structure, $\mathbf{p}(t)$ is the vector of acoustic pressures, $\mathbf{M}_s$ is the mass matrix of the structure, $\mathbf{M}_a$ is called "mass" matrix of acoustic fluid (its components are not homogeneous to masses, the name is chosen for analogy with structural denomination), $\mathbf{K}_s$ is the stiffness matrix of the structure, $\mathbf{K}_a$ is the "stiffness" matrix of fluid domain, $\mathbf{L}$ is the vibroacoustic coupling matrix, $\mathbf{C}_s$ and $\mathbf{C}_a$ respectively represent structural and acoustic losses. This formulation includes the hypothesis that there is no loss at the coupling between structural and acoustic parts, and that internal losses can be represented using equivalent viscous models. $\mathbf{F}_s(t)$ is the vector representing the generalized forces on the structure, while $\dot{\mathbf{Q}}_a(t)$ is associated to acoustic sources (volume acceleration) in the cavity.

The non-self-adjoint character of the formulation induces difficulties for the resolution of this kind of problem using modal decomposition. Some research works have been done to find symmetric formulations dedicated to coupled vibroacoustic problems [16, 29], but up to now, these formulations are either not able to take into account dissipation in the fluid domain, or lead to full matrices which can not be efficiently used for large models. The technique which is widely used for model reduction in the field of numerical analysis is based on the use of two uncoupled bases (structural and fluid), and the solution of the coupled system is projected on these bases, even if some convergence problems can be found [37]. Being able to evaluate numerically the coupled modal basis in an efficient way is still a challenge, in particular for damped problems. On the other hand, starting from experimental data, it is possible to identify these modes [39], and one of the ways to build reduced models could be to follow the same methodology as the one used in structural dynamics, extended to vibroacoustics.

11.4.2 Complex Modes for Vibroacoustics

The system (11.29) can be solved for steady-state harmonics by modal decomposition. The non-symmetric character of the matrix system implies that right and left modes must be identified. This can be done using the space-state representation of the system

$$\mathbf{U}\dot{\mathbf{Q}}(t) - \mathbf{A}\mathbf{Q}(t) = \mathbf{F}(t), \tag{11.30}$$

where

$$\mathbf{U} = \begin{bmatrix} \mathbf{C} & \mathbf{M} \\ \mathbf{M} & \mathbf{0} \end{bmatrix}, \qquad \mathbf{A} = \begin{bmatrix} -\mathbf{K} & \mathbf{0} \\ \mathbf{0} & \mathbf{M} \end{bmatrix}, \qquad \mathbf{Q}(t) = \begin{Bmatrix} \mathbf{q}(t) \\ \dot{\mathbf{q}}(t) \end{Bmatrix},$$
$$\mathbf{F}(t) = \begin{Bmatrix} \mathbf{f}(t) \\ \mathbf{0} \end{Bmatrix}. \tag{11.31}$$

The eigenvalues of this problem can be stored in the spectral matrix $\boldsymbol{\Lambda}$,

$$\boldsymbol{\Lambda} = \left[\diagdown \lambda_j \diagdown \right]. \tag{11.32}$$

The j-th eigenvalue is associated to:

- a right eigenvector, $\boldsymbol{\theta}_{\mathrm{R}j}$ such that $(\mathbf{U}\lambda_j - \mathbf{A})\boldsymbol{\theta}_{\mathrm{R}j} = \mathbf{0}$, where $\boldsymbol{\theta}_{\mathrm{R}j} = \{\psi_{\mathrm{R}j}^{\mathrm{T}}\ \psi_{\mathrm{R}j}^{\mathrm{T}}\lambda_j\}^{\mathrm{T}}$. Storing the eigenvectors (in the same order as the eigenvalues) in the modal matrix $\boldsymbol{\Theta}_{\mathrm{R}} = [\psi_{\mathrm{R}}^{\mathrm{T}}\ \boldsymbol{\Lambda}\psi_{\mathrm{R}}^{\mathrm{T}}]^{\mathrm{T}}$, the following relationship is verified,

$$\mathbf{U}\boldsymbol{\Theta}_{\mathrm{R}}\boldsymbol{\Lambda} = \mathbf{A}\boldsymbol{\Theta}_{\mathrm{R}}; \tag{11.33}$$

- a left eigenvector $\boldsymbol{\theta}_{\mathrm{L}j}$, such that $\boldsymbol{\theta}_{\mathrm{L}j}^{\mathrm{T}}(\mathbf{U}\lambda_j - \mathbf{A}) = \mathbf{0}$, where $\boldsymbol{\theta}_{\mathrm{L}j} = \{\psi_{\mathrm{L}j}^{\mathrm{T}}\ \psi_{\mathrm{L}j}^{\mathrm{T}}\lambda_j\}^{\mathrm{T}}$. Storing the eigenvectors (in the same order as the eigenvalues) in the modal matrix $\boldsymbol{\Theta}_{\mathrm{L}} = [\psi_{\mathrm{L}}^{\mathrm{T}}\ \boldsymbol{\Lambda}\psi_{\mathrm{L}}^{\mathrm{T}}]^{\mathrm{T}}$, the following relationships are verified,

$$\mathbf{U}^{\mathrm{T}}\boldsymbol{\Theta}_{\mathrm{L}}\boldsymbol{\Lambda} = \mathbf{A}^{\mathrm{T}}\boldsymbol{\Theta}_{\mathrm{L}} \quad \text{or} \quad \boldsymbol{\Lambda}\boldsymbol{\Theta}_{\mathrm{L}}^{\mathrm{T}}\mathbf{U} = \boldsymbol{\Theta}_{\mathrm{L}}^{\mathrm{T}}\mathbf{A}. \tag{11.34}$$

The orthogonality relationships can be written using $2n$ arbitrary values to build the diagonal matrix $\boldsymbol{\xi} = [\diagdown \xi_j \diagdown]$,

$$\boldsymbol{\Theta}_{\mathrm{L}}^{\mathrm{T}}\mathbf{U}\boldsymbol{\Theta}_{\mathrm{R}} = \boldsymbol{\xi} \quad \text{or} \quad \boldsymbol{\Theta}_{\mathrm{L}}^{\mathrm{T}}\mathbf{A}\boldsymbol{\Theta}_{\mathrm{R}} = \boldsymbol{\xi}\boldsymbol{\Lambda}. \tag{11.35}$$

The modal decomposition of the permanent harmonic response at frequency ω is

$$\mathbf{Q}(t) = \boldsymbol{\Theta}_{\mathrm{R}}\big(\boldsymbol{\xi}(\mathrm{i}\omega\mathbf{E}_{2n} - \boldsymbol{\Lambda})\big)^{-1}\boldsymbol{\Theta}_{\mathrm{L}}^{\mathrm{T}}\mathbf{F}(\omega)e^{\mathrm{i}\omega t}, \tag{11.36}$$

where $\mathbf{E}_{2n}$ is the $2n \times 2n$ identity matrix and $\mathbf{F}(\omega)$ is the complex amplitude of the harmonic excitation. This relationship can also be written using the n degrees of freedom notations in the frequency domain as

$$\mathbf{Q}(\omega) = \psi_{\mathrm{R}} \Xi \psi_{\mathrm{L}}^{\mathrm{T}} \mathbf{f}(\omega), \tag{11.37}$$

where

$$\Xi = \begin{bmatrix} \ddots & & \\ & \dfrac{1}{\xi_j(\mathrm{i}\omega - \lambda_j)} & \\ & & \ddots \end{bmatrix}. \tag{11.38}$$

In the following, without loss of generality, the eigenshapes are supposed to be normalized such that $\xi_j = 1$.

Each mode has its own response which is proportional to the right eigenvector, with a modal participation vector that includes the scalar product between the left eigenvector and the force exciting the system. In the case of a self-adjoint problem, right and left eigenvectors are equal. The non-self adjoint character of problem (11.1) is particular since extradiagonal coupling terms that appear in mass and stiffness matrices are linked. It can be shown [39] that the left eigenvectors are related to the right ones by the following relationship:

$$\text{If } \psi_{\mathrm{R}j} = \begin{Bmatrix} \mathbf{X}_j \\ \mathbf{P}_j \end{Bmatrix} \quad \text{then } \psi_{\mathrm{L}j} = \begin{Bmatrix} \mathbf{X}_j \\ -\mathbf{P}_j \lambda_j^{-2} \end{Bmatrix}, \tag{11.39}$$

where X corresponds to the structural dofs of the eigenvectors, and P is related to the acoustic dofs. This point is fundamental for modal analysis of coupled system, since only extraction of right eigenvectors is required to derive the left ones. The previous relation can also be written as

$$\text{If } \psi_{\mathrm{R}} = \begin{bmatrix} \mathbf{X} \\ \mathbf{P} \end{bmatrix} \quad \text{then } \psi_{\mathrm{L}} = \begin{bmatrix} \mathbf{X} \\ -\mathbf{P}\boldsymbol{\Lambda}^{-2} \end{bmatrix}. \tag{11.40}$$

11.4.3 Properness for Vibroacoustics

The properness condition in the case of a non-self adjoint system can be derived from the orthogonality relationships (11.35):

$$\mathbf{U}^{-1} = \boldsymbol{\Theta}_{\mathrm{R}} \boldsymbol{\Theta}_{\mathrm{L}}^{\mathrm{T}}, \tag{11.41}$$

or

$$\begin{aligned} \begin{bmatrix} \mathbf{C} & \mathbf{M} \\ \mathbf{M} & \mathbf{0} \end{bmatrix}^{-1} &= \begin{bmatrix} \mathbf{0} & \mathbf{M}^{-1} \\ \mathbf{M}^{-1} & -\mathbf{M}^{-1}\mathbf{C}\mathbf{M}^{-1} \end{bmatrix} \\ &= \begin{bmatrix} \psi_{\mathrm{R}}\psi_{\mathrm{L}}^{\mathrm{T}} & \psi_{\mathrm{R}}\boldsymbol{\Lambda}\psi_{\mathrm{L}}^{\mathrm{T}} \\ \psi_{\mathrm{R}}\boldsymbol{\Lambda}\psi_{\mathrm{L}}^{\mathrm{T}} & \psi_{\mathrm{R}}\boldsymbol{\Lambda}^2\psi_{\mathrm{L}}^{\mathrm{T}} \end{bmatrix}, \end{aligned} \tag{11.42}$$

and

$$\mathbf{A}^{-1} = \boldsymbol{\Theta}_{\mathrm{R}} \boldsymbol{\Lambda} \boldsymbol{\Theta}_{\mathrm{L}}^{\mathrm{T}}, \tag{11.43}$$

or

$$\begin{bmatrix} -\mathbf{K} & \mathbf{0} \\ \mathbf{0} & \mathbf{M} \end{bmatrix}^{-1} = \begin{bmatrix} -\mathbf{K}^{-1} & \mathbf{0} \\ \mathbf{0} & \mathbf{M}^{-1} \end{bmatrix} = \begin{bmatrix} \psi_{\mathrm{R}}\mathbf{\Lambda}^{-1}\psi_{\mathrm{L}}^{\mathrm{T}} & \psi_{\mathrm{R}}\psi_{\mathrm{L}}^{\mathrm{T}} \\ \psi_{\mathrm{R}}\psi_{\mathrm{L}}^{\mathrm{T}} & \psi_{\mathrm{R}}\mathbf{\Lambda}\psi_{\mathrm{L}}^{\mathrm{T}} \end{bmatrix}. \tag{11.44}$$

It is then clear that the properness condition for a non-symmetric second order system can be written as

$$\psi_{\mathrm{R}}\psi_{\mathrm{L}}^{\mathrm{T}} = \mathbf{0}. \tag{11.45}$$

Once this relationship is verified, the matrices can be found using the inverse relations

$$\mathbf{M} = \left[\psi_{\mathrm{R}}\mathbf{\Lambda}\psi_{\mathrm{L}}^{\mathrm{T}}\right]^{-1}, \tag{11.46}$$

$$\mathbf{K} = -\left[\psi_{\mathrm{R}}\mathbf{\Lambda}^{-1}\psi_{\mathrm{L}}^{\mathrm{T}}\right]^{-1}, \tag{11.47}$$

$$\mathbf{C} = -\left[\mathbf{M}\psi_{\mathrm{R}}\mathbf{\Lambda}^{2}\psi_{\mathrm{L}}^{\mathrm{T}}\mathbf{M}\right]. \tag{11.48}$$

For the particular vibroacoustic case, left eigenvectors are linked to right ones, and the properness condition can be written using only the right complex eigenvectors,

$$\begin{bmatrix} \mathbf{X}\mathbf{X}^{\mathrm{T}} & -\mathbf{X}\mathbf{\Lambda}^{-2}\mathbf{P}^{\mathrm{T}} \\ \mathbf{P}\mathbf{X}^{\mathrm{T}} & -\mathbf{P}\mathbf{\Lambda}^{-2}\mathbf{P}^{\mathrm{T}} \end{bmatrix} = \mathbf{0}. \tag{11.49}$$

11.4.4 Methodologies for Properness Enforcement

11.4.4.1 Structural Dynamics Based Strategy

When the complex modes are available from experimental identification, one can use Eqs. (11.46) to (11.48) in order to find the reduced model which is supposed to have the same behavior as the measured one. The fact is that in general, the modes do not verify the properness condition (11.49). In the particular case of vibroacoustics, one can try to follow the same methodology as the one used in structural dynamics. The following constrained optimization problem should then be solved:

$$\begin{aligned} &\text{Find } \tilde{\mathbf{X}} \text{ and } \tilde{\mathbf{P}} \text{ minimizing } \|\tilde{\mathbf{X}}-\mathbf{X}\| \text{ and } \|\tilde{\mathbf{P}}-\mathbf{P}\| \\ &\text{while} \\ &\tilde{\mathbf{X}}\tilde{\mathbf{X}}^{\mathrm{T}} = \mathbf{0}, \quad \tilde{\mathbf{X}}\tilde{\mathbf{P}}^{\mathrm{T}} = \mathbf{0}, \quad \tilde{\mathbf{X}}\mathbf{\Lambda}^{-2}\tilde{\mathbf{P}}^{\mathrm{T}} = \mathbf{0}, \quad \tilde{\mathbf{P}}\mathbf{\Lambda}^{-2}\tilde{\mathbf{P}}^{\mathrm{T}} = \mathbf{0}, \end{aligned} \tag{11.50}$$

where $\mathbf{X}$ and $\mathbf{P}$ are two given complex rectangular matrices and $\mathbf{\Lambda}$ is a given diagonal complex matrix. This problem can be re-written using 4 Lagrange multipliers matrices $\boldsymbol{\delta}_j$ ($j = 1$ to 4), yielding

$$
\begin{aligned}
&\begin{Bmatrix} \tilde{\mathbf{X}} \\ \tilde{\mathbf{P}} \end{Bmatrix} - \begin{Bmatrix} \mathbf{X} \\ \mathbf{P} \end{Bmatrix} + \frac{1}{2}\begin{bmatrix} \boldsymbol{\delta}_1 + \boldsymbol{\delta}_1^{\mathrm{T}} & \boldsymbol{\delta}_2 \\ \boldsymbol{\delta}_2^{\mathrm{T}} & \mathbf{0} \end{bmatrix} \begin{Bmatrix} \overline{\tilde{\mathbf{X}}} \\ \overline{\tilde{\mathbf{P}}} \end{Bmatrix} \\
&\qquad - \frac{1}{2}\begin{bmatrix} \mathbf{0} & \boldsymbol{\delta}_3 \\ \boldsymbol{\delta}_3^{\mathrm{T}} & \boldsymbol{\delta}_4 + \boldsymbol{\delta}_4^{\mathrm{T}} \end{bmatrix} \begin{Bmatrix} \overline{\tilde{\mathbf{X}}\boldsymbol{\Lambda}^{-2}} \\ \overline{\tilde{\mathbf{P}}\boldsymbol{\Lambda}^{-2}} \end{Bmatrix} = \mathbf{0}, \\
&\tilde{\mathbf{X}}\tilde{\mathbf{X}}^{\mathrm{T}} = \mathbf{0}, \\
&\tilde{\mathbf{X}}\tilde{\mathbf{P}}^{\mathrm{T}} = \mathbf{0}, \\
&\tilde{\mathbf{X}}\boldsymbol{\Lambda}^{-2}\tilde{\mathbf{P}}^{\mathrm{T}} = \mathbf{0}, \\
&\tilde{\mathbf{P}}\boldsymbol{\Lambda}^{-2}\tilde{\mathbf{P}}^{\mathrm{T}} = \mathbf{0},
\end{aligned}
\tag{11.51}
$$

where the overbars correspond to complex conjugates. Solving this problem is clearly not easy because of the presence of the $\boldsymbol{\Lambda}$ matrices that makes impossible to find explicitly the expression of multipliers versus the unknown vectors. An iterative procedure could be investigated but this is not the best way to obtain quick results that can be used in real-time during modal analysis. Some simplified methods have been proposed [30], among which one is called over-properness: considering the fact that the method developed for structural dynamics [7] is valid for all matrix $\mathbf{Y}$ subjected to a properness condition $\mathbf{Y}\mathbf{Y}^{\mathrm{T}} = \mathbf{0}$, one can use as $\mathbf{Y}$ matrix:

$$
\mathbf{Y} = \begin{bmatrix} \mathbf{X} \\ \mathbf{P} \\ -\mathbf{P}\boldsymbol{\Lambda}^{-2} \end{bmatrix}, \tag{11.52}
$$

yielding

$$
\mathbf{Y}\mathbf{Y}^{\mathrm{T}} = \begin{bmatrix} \mathbf{X}\mathbf{X}^{\mathrm{T}} & \mathbf{X}\mathbf{P}^{\mathrm{T}} & -\mathbf{X}\boldsymbol{\Lambda}^{-2}\mathbf{P}^{\mathrm{T}} \\ \mathbf{P}\mathbf{X}^{\mathrm{T}} & \mathbf{P}\mathbf{P}^{\mathrm{T}} & -\mathbf{P}\boldsymbol{\Lambda}^{-2}\mathbf{P}^{\mathrm{T}} \\ -\mathbf{P}\boldsymbol{\Lambda}^{-2}\mathbf{X}^{\mathrm{T}} & -\mathbf{P}\boldsymbol{\Lambda}^{-2}\mathbf{P}^{\mathrm{T}} & \mathbf{P}\boldsymbol{\Lambda}^{-4}\mathbf{P}^{\mathrm{T}} \end{bmatrix}. \tag{11.53}
$$

It can be observed that the four required terms of Eq. (11.49) are included in this matrix, while two of them are not theoretically required. Using this vector in the procedure detailed by Eqs. (11.18)–(11.20) leads to a so-called over-proper solution which includes more constraints than those required, but that includes the required ones.

11.4.4.2 Alternative Strategy

Another thinkable way for obtaining matrices of system (11.29) is to use a least-square approach. Being given a set of measured frequency responses $\mathbf{X}$ corresponding to a set of measured excitations $\mathbf{F}$, the matrices can be found by solving the minimization problem

$$
\min_{(\mathbf{M},\mathbf{C},\mathbf{K})\in\mathbb{A}} \varepsilon(\mathbf{M},\mathbf{C},\mathbf{K}) = \left\| \left(-\omega^2\mathbf{M} + \mathrm{i}\omega\mathbf{C} + \mathbf{K}\right)\mathbf{X} = \mathbf{F} \right\|, \tag{11.54}
$$

where $\mathbb{A} = \mathbb{M} \times \mathbb{C} \times \mathbb{K}$ is the space of admissible matrices (whose topology correspond to a vibroacoustic problem). The function to minimize can be written using a linear system,

$$\varepsilon(\mathbf{M}, \mathbf{C}, \mathbf{K}) = \|\mathbf{D}\boldsymbol{\alpha} - \mathbf{G}\|, \tag{11.55}$$

where $\boldsymbol{\alpha} = \{M_{11} M_{12} \ldots K_{nn}\}^{\mathrm{T}}$, while $\mathbf{D}$ includes terms coming from $\mathbf{X}$ and ω, and $\mathbf{G}$ includes terms coming from $\mathbf{F}$. The matrices components can finally be found using pseudo-inverse for minimization of least-square error,

$$\boldsymbol{\alpha} = \left(\mathbf{D}^{\mathrm{T}}\mathbf{D}\right)^{-1}\mathbf{D}\mathbf{G}. \tag{11.56}$$

This strategy can then be used to directly find the matrices without using the complex eigenvectors, which can be found in post processing stage by solving the eigenvalue problem. This approach implies undoubtedly a higher calculation cost than the previous strategies, in particular for systems with numerous degrees of freedom, while in the case of low order reduced models, this strategy could be appropriate.

11.4.5 Numerical Illustration

The strategies which have been proposed here can be compared with a direct matrices reconstruction, i.e. without properness enforcement. The first test-case which is proposed here is a very simple 2-dofs numerical model, whose topology is the same as the one given in Eq. (11.29):

$$\begin{bmatrix} 3.23 & 0 \\ -1.46 & 1.27 \times 10^{-2} \end{bmatrix} \begin{Bmatrix} \ddot{x} \\ \ddot{p} \end{Bmatrix} + \begin{bmatrix} 1.12 & 0 \\ 0 & 3.18 \times 10^{-3} \end{bmatrix} \begin{Bmatrix} \dot{x} \\ \dot{p} \end{Bmatrix} + \begin{bmatrix} 1000 & 1.46 \\ 0 & 1.65 \end{bmatrix} \begin{Bmatrix} x \\ p \end{Bmatrix} = \begin{Bmatrix} F(t) \\ \dot{Q}_a(t) \end{Bmatrix}. \tag{11.57}$$

Starting from this system, the complex eigenmodes are evaluated. Some noise is then added to the eigenfrequencies and eigenvectors (5% random noise on frequency, 10% on mode shapes), and the matrices of the system are evaluated using the three approaches:

- direct reconstruction from complex modes (without properness enforcement);
- reconstruction from complex modes (with over-properness enforcement);
- reconstruction from least-square error on FRFs (the FRFs being generated with the noisy eigenvalues in order to keep the same noise level).

Finally, the three results are compared by comparing the reconstructed matrices to the original ones (when available) or by plotting FRFs evaluated using each set of matrices.

The direct approach, which is exact if no error exists in the identification procedure, is clearly very sensitive to noise, and final matrices can be very different from expected results. The corresponding matrices are:

$$\mathbf{M} = \begin{bmatrix} 3.29 & -4.00 \times 10^{-4} \\ -1.55 & 1.31 \times 10^{-2} \end{bmatrix}, \qquad \mathbf{C} = \begin{bmatrix} -1.53 & -1.02 \times 10^{-2} \\ -1.28 & 6.10 \times 10^{-3} \end{bmatrix}, \tag{11.58}$$
$$\mathbf{K} = \begin{bmatrix} 964 & 1.37 \\ -14.1 & 1.66 \end{bmatrix}.$$

Estimation of mass and stiffness matrices is quite good, while the damping matrix is very badly reconstructed. Some clear improvements can be observed when the properness is enforced. The stiffness and mass matrices are almost unchanged, while the physical meaning of the damping matrix is improved when it is derived from the corrected eigenvectors:

$$\mathbf{M} = \begin{bmatrix} 3.30 & -4.12 \times 10^{-4} \\ -1.55 & 1.31 \times 10^{-2} \end{bmatrix}, \qquad \mathbf{C} = \begin{bmatrix} 2.62 & -5.04 \times 10^{-3} \\ -0.653 & -1.21 \times 10^{-4} \end{bmatrix}, \tag{11.59}$$
$$\mathbf{K} = \begin{bmatrix} 965 & 1.37 \\ -14.5 & 1.66 \end{bmatrix}.$$

The negative damping term on the fluid part is balanced with its very small value compared to the (positive) value on the structural part. Finally, the least-square error (LSE) approach leads to a correct topology of matrices, with physical damping terms on both structural and acoustic parts:

$$\mathbf{M} = \begin{bmatrix} 3.31 & 0 \\ -1.44 & 1.27 \times 10^{-2} \end{bmatrix}, \qquad \mathbf{C} = \begin{bmatrix} 0.740 & 0 \\ 0 & 4.12 \times 10^{-3} \end{bmatrix}, \tag{11.60}$$
$$\mathbf{K} = \begin{bmatrix} 982 & 1.44 \\ 0 & 1.62 \end{bmatrix}.$$

The three strategies can be compared using one of the corresponding FRFs in Fig. 11.11, on which the bad behavior of the direct method can be observed. One can also observe that, even if the topology of the over-proper solution is not exactly the right one, the global error on FRFs reconstruction is lower than in the case of LSE technique. Indeed, depending on the objective, one should evaluate matrices from both formulations and choose the ones which are the most appropriate.

11.4.6 Experimental Test-Case

The second test-case which is proposed here corresponds to an experimental test-case based on measurements on a guitar given by F. Gautier from LAUM-Le Mans and J.-L. Le Carrou from LAM-Paris VI. In that case, only two degrees of freedom are considered, in order to represent the behavior of the guitar in the frequency range corresponding to the so-called A0 and T1 modes, which are of first interest in the design of the instrument [13, 18, 25]. The two degrees of freedom which have been

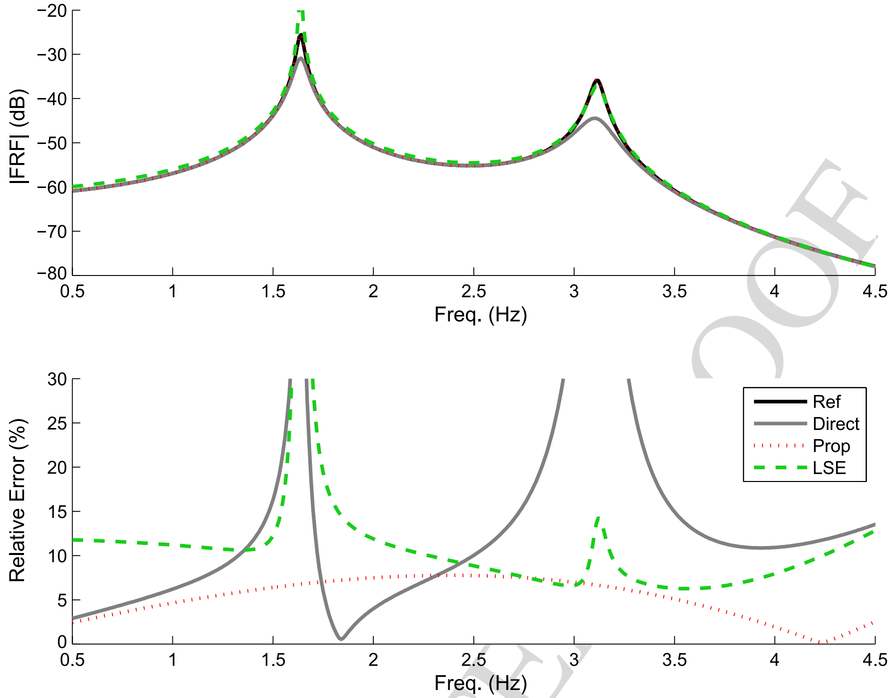

Fig. 11.11 Methodologies for properness enforcement on numerical test-case

used in these measurements correspond to the structural transverse displacement of a point on the soundboard, and the acoustic pressure in the middle of the sound hole. A small impact hammer has been used for excitation on the structural degree of freedom. These two modes have been identified experimentally by a curve fitting technique, and the FRFs built from these two modes is considered as the reference in the following. The direct approach leads once again to bad estimation of damping terms:

$$\mathbf{M} = \begin{bmatrix} 3.10\times 10^{-2} & 2.10\times 10^{-9} \\ 3.88\times 10^{-2} & 2.85\times 10^{-7} \end{bmatrix}, \qquad \mathbf{C} = \begin{bmatrix} -2.23 & 2.19\times 10^{-6} \\ -3.68 & -3.72\times 10^{-5} \end{bmatrix}, \tag{11.61}$$
$$\mathbf{K} = \begin{bmatrix} 2.30\times 10^{4} & -3.59\times 10^{-3} \\ 705 & 1.28\times 10^{-5} \end{bmatrix}.$$

The properness enforcement allows the damping terms to become more physical:

$$\mathbf{M} = \begin{bmatrix} 3.09\times 10^{-2} & 1.88\times 10^{-9} \\ 3.84\times 10^{-2} & 2.83\times 10^{-7} \end{bmatrix}, \qquad \mathbf{C} = \begin{bmatrix} 0.942 & -1.52\times 10^{-6} \\ 0.315 & 7.55\times 10^{-6} \end{bmatrix}, \tag{11.62}$$
$$\mathbf{K} = \begin{bmatrix} 2.27\times 10^{4} & -3.57\times 10^{-3} \\ 632 & 1.26\times 10^{-5} \end{bmatrix}.$$

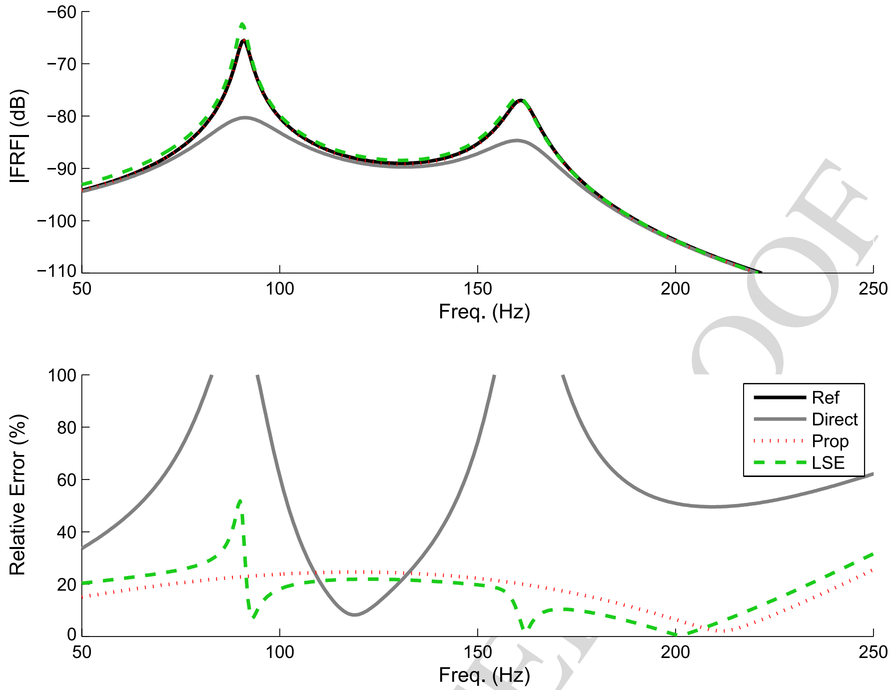

Fig. 11.12 Methodologies for properness enforcement on guitar measurements

Finally, the least-square error (LSE) approach leads to a correct topology of matrices, with physical damping term on structural part, but not on the acoustic part:

$$\mathbf{M} = \begin{bmatrix} 2.91 \times 10^{-2} & 0 \\ 3.44 \times 10^{-2} & 2.57 \times 10^{-7} \end{bmatrix}, \qquad \mathbf{C} = \begin{bmatrix} 1.37 & 0 \\ 0 & -2.97 \times 10^{-6} \end{bmatrix},$$
$$\mathbf{K} = \begin{bmatrix} 2.15 \times 10^{4} & -3.45 \times 10^{-3} \\ 0 & 1.15 \times 10^{-5} \end{bmatrix}. \tag{11.63}$$

The comparison of FRFs, in Fig. 11.12, leads to the conclusions in accordance with both structural application and vibroacoustical numerical test-case. One can point out the fact that all methodologies lead to quite good estimation of mass and stiffness matrices, the critical point being the evaluation of damping matrix. The properness enforcement is not sufficient to obtain the correct topology, but the improvement is nevertheless clear, it can be seen as a regularization procedure for the inverse problem which is addressed here.

11.5 Prospects for the Future

As far as the structural dynamics applications are concerned, the properness enforcement technique leads to optimal complex modes that can be derived from identified ones. These modes can be efficiently used to reconstruct the system matrices when the full set of vectors is available. This should be considered in any application, since this operation acts as a regularization and helps to identify physical damping matrices. A challenge for the future is clearly to extend this notion for an incomplete set of identified complex vectors.

Concerning the vibroacoustic extension, the properness condition has been derived. In this case no explicit solution can be found, obtaining optimal complex modes that verify the properness condition is still a challenge. Of course constrained minimization techniques could be applied, but they would certainly lead to a high calculation cost. The efficiency of the approach in the context of structural dynamics leads to similar expectations for the vibroacoustic case. Nevertheless some more research in this way are required to provide an efficient tool that works in any situation. The alternative way to achieve the expected goal is to extend advanced FRF-based methods referenced in the chapter to vibroacoustic applications. This could possibly lead to good results, since the least-square technique proposed here based on FRF data gives interesting results. This is undoubtedly a promising way to obtain efficient reconstruction of reduced vibroacoustic models.

11.6 Summary

Damping matrices identification in the context of structural dynamics, starting from a full modal basis identified by measurements, is a topic which is quite clear today. The inverse procedure is very sensitive to noise on input data (i.e. on identified complex vectors), and some methods are available to provide regularization techniques based on physical considerations. Among them, the properness enforcement technique is undoubtedly very efficient, as shown on illustrative examples.

The properness condition can be easily extended to vibroacoustics: this property must be verified by complex modes in order to be those of a physical system. Two techniques have been proposed to enforce the property on eigenshapes that do not verify it, leading to much better results than those corresponding to the use of initial identified vectors. The first technique is based on the structural dynamics procedure, leading to enforcement of more conditions than the theoretically required ones. The second one is based on a least square error minimization. None of the two methods exhibits perfect results, so it is clear that one of the next challenges in vibroacoustic reduced models identification based on experimental modal analysis will be the improvement of the properness enforcement methodology. Up to now, the two proposed methods can be applied for a given application and the user can choose between results depending of the efficiency of the identified reduced model.

11.7 Selected Bibliography

For a deeper insight into damping identification techniques, the following references are suggested. Adhikari and Woodhouse have written a very well documented paper in 4 parts [3–6], which constitutes a starting point for understanding the context and methodologies available for damping identification.

The paper from Lin and Zhu [27] can be referenced as a good illustration of the relationship between viscous and hysteretic damping models, in particular to understand that viscous and hysteretic damping matrices are almost equivalent when the damping is distributed on the structure, while a correct choice of the damping model is of first importance for systems with distributed damping.

In this context, Xu [40] has proposed an interesting formulation for computing explicit damping matrices for multiply connected, non-classically damped, coupled systems.

It is nevertheless clear that most of the methodologies have been developed for viscous or proportional damping. In particular, the paper from Barbieri et al. [8] gives a comparison of three techniques for identification of proportional damping matrix of transmission line cables, and the paper from Pilkey et al. [32], dedicated to viscous damping, investigates some aspects of the damping identification procedure that are noise, spatial incompleteness and modal incompleteness.

There are few papers to which the reader is invited to refer concerning identification of non-proportional damping, among which those by Adhikari [2] and Kasai and Link [23].

Almost all the methods that allows identification of damping matrix are related to measurements dofs: the size of the identified matrix is equal to the number of measurement points. The paper from Ozgen and Kim [31] compares two methods that can be used to expand the experimental damping matrix to the size of the analytical model.

Acknowledgements The authors would like to thank Jean-Loïc Le Carrou from Laboratoire d'Acoustique Musicale (Paris VI) and François Gautier from the Laboratoire d'Acoustique de l'Université du Maine, for the fruitful discussions and for allowing us to use their measurements data, used in the last part of the chapter.

References

1. Adhikari, S.: Optimal complex modes and an index of damping non-proportionality. Mech. Syst. Signal Process. **18**(1), 1–28 (2004)
2. Adhikari, S.: Damping modelling using generalized proportional damping. J. Sound Vib. **293**(1–2), 156–170 (2006)
3. Adhikari, S., Woodhouse, J.: Identification of damping: Part 1, viscous damping. J. Sound Vib. **243**(1), 43–61 (2001)
4. Adhikari, S., Woodhouse, J.: Identification of damping: Part 2, non-viscous damping. J. Sound Vib. **243**(1), 63–88 (2001)
5. Adhikari, S., Woodhouse, J.: Identification of damping: Part 3, symmetry-preserving methods. J. Sound Vib. **251**(3), 477–490 (2002)

6. Adhikari, S., Woodhouse, J.: Identification of damping: Part 4, error analysis. J. Sound Vib. **251**(3), 491–504 (2002)
7. Balmès, E.: New results on the identification of normal modes from experimental complex ones. Mech. Syst. Signal Process. **11**(2), 229–243 (1997)
8. Barbieri, N., Souza Júnior, O.H., Barbieri, R.: Dynamical analysis of transmission line cables. Part 2—damping estimation. Mech. Syst. Signal Process. **18**(3), 671–681 (2004)
9. Bernal, D., Gunes, B.: Extraction of second order system matrices from state space realizations. In: 14th ASCE Engineering Mechanics Conference (EM2000), Austin, Texas (2000)
10. Bert, C.W.: Material damping: An introductory review of mathematic measures and experimental technique. J. Sound Vib. **29**(2), 129–153 (1973)
11. Caughey, T.K., O'Kelly, M.E.: Classical normal modes in damped linear systems. J. Appl. Mech. **32**, 583–588 (1965)
12. Chen, S.Y., Ju, M.S., Tsuei, Y.G.: Estimation of mass, stiffness and damping matrices from frequency response functions. J. Vib. Acoust. **118**(1), 78–82 (1996)
13. Christensen, O., Vistisen, B.B.: Simple model for low frequency guitar function. J. Acoust. Soc. Am. **68**(3), 758–766 (1980)
14. Craig, R.J., Bampton, M.: Coupling of substructures for dynamic analyses. AIAA J. **6**(7), 1313–1319 (1968)
15. Crandall, S.H.: The role of damping in vibration theory. J. Sound Vib. **11**(1), 3–18 (1970)
16. Everstine, G.C. Finite element formulations of structural acoustics problems. Comput. Struct. **65**(3), 307–321 (1997)
17. Fillod, R., Piranda, J.: Research method of the eigenmodes and generalized elements of a linear mechanical structure. Shock Vib. Bull. **48**(3), 5–12 (1978)
18. Fletcher, N.H., Rossing, T.D.: The Physics of Musical Instruments. Springer, Berlin (1998)
19. Fritzen, C.P.: Identification of mass, damping, and stiffness matrices of mechanical systems. J. Vib. Acoust. Stress Reliab. Des. **108**, 9–16 (1986)
20. Gaul, L.: The influence of damping on waves and vibrations. Mech. Syst. Signal Process. **13**(1), 1–30 (1999)
21. Ibrahim, S.R.: Dynamic modeling of structures from measured complex modes. AIAA J. **21**(6), 898–901 (1983)
22. Ibrahim, S.R., Sestieri, A.: Existence and normalization of complex modes in post experimental use in modal analysis. In 13th International Modal Analysis Conference, Nashville, USA, pp. 483–489 (1995)
23. Kasai, T., Link, M.: Identification of non-proportional modal damping matrix and real normal modes. Mech. Syst. Signal Process. **16**(6), 921–934 (2002)
24. Lancaster, P., Prells, U.: Inverse problems for damped vibrating systems. J. Sound Vib. **283**(3–5), 891–914 (2005)
25. Le Carrou, J.-L., Gautier, F., Foltête, E.: Experimental study of A0 and T1 modes of the concert harp. J. Acoust. Soc. Am. **121**(1), 559–567 (2007)
26. Lee, J.H., Kim, J.: Development and validation of a new experimental method to identify damping matrices of a dynamic system. J. Sound Vib. **246**(3), 505–524 (2001)
27. Lin, R.M., Zhu, J.: On the relationship between viscous and hysteretic damping models and the importance of correct interpretation for system identification. J. Sound Vib. **325**(1–2), 14–33 (2009)
28. Minas, C., Inman, D.J.: Identification of a nonproportional damping matrix from incomplete modal information. J. Vib. Acoust. **113**(2), 219–224 (1991)
29. Morand, H.J.-P., Ohayon, R.: Fluid Structure Interaction. Wiley, New York (1995)
30. Ouisse, M., Foltête, E.: On the comparison of symmetric and unsymmetric formulations for experimental vibro-acoustic modal analysis. In: Acoustics'08, Paris, 2008
31. Ozgen, G.O., Kim, J.H.: Direct identification and expansion of damping matrix for experimental-analytical hybrid modeling. J. Sound Vib. **308**(1–2), 348–372 (2007)
32. Pilkey, D.F., Park, G., Inman, D.J.: Damping matrix identification and experimental verification. In: Smart Structures and Materials, SPIE Conference on Passive Damping and Isolation, Newport Beach, California, pp. 350–357 (1999)

33. Prandina, M., Mottershead, J.E., Bonisoli, E.: An assessment of damping identification methods. J. Sound Vib. **323**(3–5), 662–676 (2009)
34. Rayleigh, J.W.S. The Theory of Sound, vols. 1, 2. Dover, New York (1945)
35. Srikantha Phani A., Woodhouse, J.: Viscous damping identification in linear vibration. J. Sound Vib. **303**(3–5), 475–500 (2007)
36. Srikantha Phani A., Woodhouse, J.: Experimental identification of viscous damping in linear vibration. J. Sound Vib. **319**(3–5), 832–849 (2009)
37. Tran, Q.H., Ouisse, M., Bouhaddi, N.: A robust component mode synthesis method for stochastic damped vibroacoustics. Mech. Syst. Signal Process. **24**(1), 164–181 (1997)
38. Van der Auweraer, H., Guillaume, P., Verboven, P., Vanlanduit, S.: Application of a fast-stabilizing frequency domain parameter estimation method. J. Dyn. Syst. Meas. Control **123**(4), 651–658 (2001)
39. Wyckaert, K., Augusztinovicz, F., Sas, P.: Vibro-acoustical modal analysis: reciprocity, model symmetry and model validity. J. Acoust. Soc. Am. **100**(5), 3172–3181 (1996)
40. Xu, J.: A synthesis formulation of explicit damping matrix for non-classically damped systems. Nucl. Eng. Des. **227**(2), 125–132 (2004)
41. Zhang, Q., Lallement, G.: Comparison of normal eigenmodes calculation methods based on identified complex eigenmodes. J. Spacecr. Rockets **24**, 69–73 (1987)